

Article

An In Situ Prepared Comb-like Polycaprolactone-Based Gel Electrolyte for High-Performance Lithium Metal Batteries

Yange Fan ^{1,2,*}, Huifeng Wang ¹, Shipeng Chen ¹ , Yimin Hou ¹ and Shujiang Wang ¹¹ Institute of Chemistry Co., Ltd., Henan Academy of Sciences, Zhengzhou 450002, China² School of Materials Science and Engineering, Zhengzhou University, Zhengzhou 450001, China

* Correspondence: fanyange@gs.zzu.edu.cn

Abstract: Herein, we present the synthesis and electrochemical performance of a comb-like polycaprolactone-based gel electrolyte from acrylate terminated polycaprolactone oligomers and liquid electrolyte for high-voltage lithium metal batteries. The ionic conductivity of this gel electrolyte at room temperature was measured to be $8.8 \times 10^{-3} \text{ S cm}^{-1}$, which is an exceptionally high value that is more than sufficient for the stable cycling of solid-state lithium metal batteries. The Li^+ transference number was detected to be 0.45, facilitating the prohibition of concentration gradients and polarization, thereby prohibiting lithium dendrite formation. In addition, the gel electrolyte exhibits high oxidation voltage up to 5.0 V vs. Li^+/Li and perfect compatibility against metallic lithium electrodes. The superior electrochemical properties provide the LiFePO_4 -based solid-state lithium metal batteries with excellent cycling stability, displaying a high initial discharge capacity of 141 mAh g^{-1} and an extraordinary capacity retention exceeding 74% of its initial specific capacity after being cycled for 280 cycles at 0.5C at room temperature. This paper presents a simple and effective in situ preparation process yielding an excellent gel electrolyte for high-performance lithium metal battery applications.

Keywords: gel electrolyte; in situ preparation; comb-like polycaprolactone; lithium metal batteries



Citation: Fan, Y.; Wang, H.; Chen, S.; Hou, Y.; Wang, S. An In Situ Prepared Comb-like Polycaprolactone-Based Gel Electrolyte for High-Performance Lithium Metal Batteries. *Materials* **2023**, *16*, 2117. <https://doi.org/10.3390/ma16052117>

Academic Editor: Satyam Panchal

Received: 6 February 2023

Revised: 1 March 2023

Accepted: 2 March 2023

Published: 6 March 2023



Copyright: © 2023 by the authors. Licensee MDPI, Basel, Switzerland. This article is an open access article distributed under the terms and conditions of the Creative Commons Attribution (CC BY) license (<https://creativecommons.org/licenses/by/4.0/>).

1. Introduction

Secondary lithium-ion batteries (LIBs) are widely employed as a sustainable energy source for applications in energy conservation devices such as portable electronics, electric vehicles (EVs), etc. [1]. However, limitations, such as restricted energy density and safety risks seriously hinder the full realization of the potential of LIBs in emerging applications of EVs and power grids. To achieve higher energy density, the use of metallic lithium as anodes is favored, owing to its extraordinary theoretical capacity (3860 mAh g^{-1}) and superior redox voltage (-3.04 V) [2]. Unfortunately, the widely used traditional organic liquid electrolytes (LEs) are limited because of their high flammability and high reactivity with metallic lithium, which result in hazardous incidents [3]. To address this challenge, the development of solid-state lithium metal batteries with solid-state electrolytes (SSE) instead of traditional LEs has emerged as an important strategy that offers improved energy and safety [4]. Given the key role of solid-state lithium batteries, polymer-based solid-state electrolytes are widely considered superior to inorganic solid-state electrolytes due to their favorable properties, including good processability, high elasticity, and perfect interfacial self-adjusting with electrodes [5,6].

Significant efforts have been invested in the development of advanced solid-state polymer electrolytes [7]. A wide range of polymer matrices have been explored for SPEs, including polyethylene oxide [8], polycarbonate [9,10], polyacrylonitrile [11], poly(vinylidene fluoride) [12], etc. Despite these efforts, solid-state polymer electrolytes are often characterized by insufficient ionic conductivity at ambient temperatures ($<10^{-5} \text{ S cm}^{-1}$) and high interfacial impedance [8,13], resulting in insufficient cycling stability and poor operational performance. Their inadequate ionic conductivity at room temperature is mainly

attributed to the semicrystalline nature of these polymer main chains and restricted segmental motions [8–10]. Various strategies have been developed to enhance ionic conductivity, such as the incorporation of inorganic additives [14], blending [15], copolymerization [16], crosslinking [17], etc. However, low ionic conductivity at ambient temperatures remains a significant barrier to the practical application of solid-state polymer electrolytes. In addition, the uncontrolled growth of lithium dendrites represents a constraint to the practical application of lithium metal batteries [18]. Therefore, the development of novel high-performance, polymer-based, solid-state electrolytes that provide sufficient electrochemical properties for lithium batteries is a hot research area in the energy conservation field.

As discussed above, to date, no solid-state polymer electrolyte has been able to satisfactorily fulfill the critical requirements for lithium metal batteries, particularly with regard to insufficient ionic conductivity at ambient temperatures. Nevertheless, polymer-based gel electrolytes (GEs) have garnered significant attention in recent years due to their remarkable attributes, including high ionic conductivity, improved interfacial contacts with the electrodes, sufficient mechanical strength, and their shape-formation capabilities [19]. These properties make GEs a highly promising solution to address safety concerns and inhibit the formation of lithium dendrites in lithium metal batteries. For instance, Yang et al. successfully synthesized polyether-based GEs through the polymerization of 1,3-dioxolane, which displays remarkable non-flammability and ionic conductivity ($3.37 \times 10^{-4} \text{ S cm}^{-1}$) at room temperature [20]. In addition to demonstrating high compatibility with metallic lithium anodes, these GEs effectively suppresses the formation of lithium dendrites during lithium plating/stripping processes. Moreover, Kim et al. reported on the synthesis of highly conductive GEs by click chemistry consisting of an ionically conductive oligomer (polycaprolactone triacrylate) and an organic solvent [21]. These GEs exhibit high ionic conductivity ($2.2 \times 10^{-3} \text{ S cm}^{-1}$) at room temperature, as well as excellent cycling performance, improved thermal stability, and no organic solvent leaking risk under high pressure. GEs offer a perfect balance between the physical and chemical properties of LEs and solid-state polymer electrolytes, as they constrain LEs within the polymer matrix, providing a potential compromise between safety and feasibility through precise regulation of the content of the LEs and the polymer matrix.

Additionally, the application of in situ polymerization techniques has emerged as a highly promising approach for the preparation of GEs, as it enables the simultaneous synthesis of the polymer electrolyte and cell assembly. This obviates the laborious and environmentally detrimental procedures associated with traditional ex situ preparation and enhances the interconnection between the electrolyte and electrodes, thereby reducing contact resistance [22]. In a study reported by Duan et al., GEs were fabricated through in situ thermally initiated polymerization, which exhibited a lower interfacial resistance and elevated ionic conductivity ($2.52 \times 10^{-4} \text{ S cm}^{-1}$ at ambient temperature) compared to the ex situ prepared cells [23]. Furthermore, Chen et al. synthesized an in situ GE composed of polyethylene glycol and LiPF_6 in carbonate solvents, which manifested high electrochemical performances ($3.35 \times 10^{-3} \text{ S cm}^{-1}$ at ambient temperature; high electrochemical stability of up to 4.9 V) [24]. Lithium dendrite formation during charge-discharge cycling is effectively mitigated through the enhancement of the solid electrolyte interphase (SEI) and the outstanding contact interface.

Herein, a simple and facile approach is presented for the synthesis of a comb-like polycaprolactone-based GE from acrylate-functionalized polycaprolactone (PCL) through the utilization of an efficient thermally initiated radical polymerization technique. The chemical structure of the reactive PCL-based precursor was thoroughly confirmed by proton nuclear magnetic resonance spectroscopy ($^1\text{H NMR}$) and Fourier transform infrared spectroscopy (FTIR). A comprehensive evaluation of the electrochemical properties was performed, including assessments of ionic conductivity, lithium-ion transference number, and compatibility with metallic lithium. Solid-state lithium metal batteries comprising $\text{LiFePO}_4/\text{GE}/\text{Li}$ were assembled and subjected to evaluations at different discharge rates. Given the high ionic conductivity and excellent interface between the GE and electrodes,

the solid-state batteries exhibit extraordinary rate and cycling performances under room-temperature conditions.

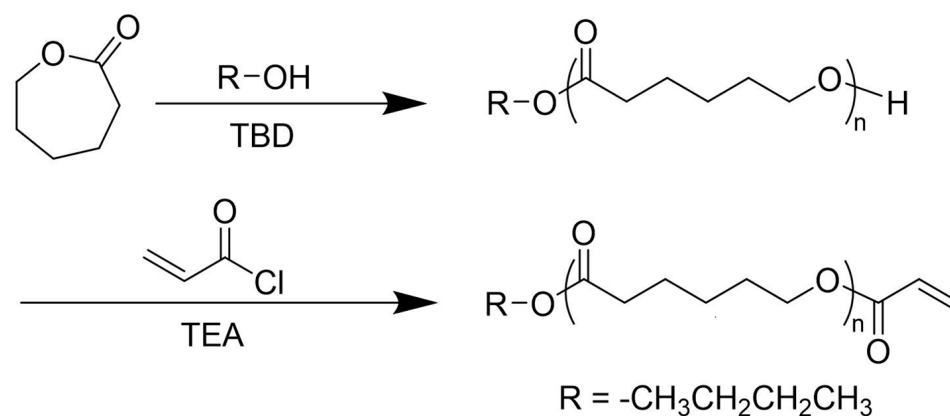
2. Experimental

2.1. Materials

The raw materials for the synthesis of acrylate-functionalized polycaprolactone oligomers, i.e., 1-butanol (99%), ϵ -caprolactone (99%), tetrahydrofuran (99%), triethylamine (97%), and toluene (99%), were all purchased from Aladdin (Shanghai, China) and dried over CaH_2 . Acryloyl chloride (96%) was obtained from Aladdin. 1,5,7-triazabicyclo[4.4.0]dec-5-ene (98%, TBD) was purchased from J&K Chemical. 2,2'-Azobis(2-methylpropionitrile) (99%, AIBN) was purchased from Aladdin and used after recrystallization in methanol. Lithium hexafluorophosphate (99.95%, LiPF_6) from Sigma Aldrich (Waltham, MA, USA) was used as the lithium salt for GE. Cathode-active materials of LiFePO_4 , carbon black (Super P), metallic Li sheets, and Al foil were purchased from Shenzhen Kejing Star Technology Co., Ltd. (Shenzhen, China). The LE used in this work was composed of ethyl methyl carbonate (EMC) and ethylene carbonate (EC) in a ratio of 7:3 (*v/v*) with 1 M LiPF_6 .

2.2. Preparation of PCLA

The synthesis of acrylate-functionalized PCL precursor (PCLA) was performed according to a previously reported literature procedure [14], as shown in Scheme 1. A typical synthetic process for PCLA is as follows: To a dry 250 mL flask, 45.66 g of ϵ -caprolactone (400 mmol), 6.67 g of 1-butanol (90 mmol), 0.28 g of TBD (2 mmol), and 100 mL of toluene were added. After degassing and refilling with Ar, the reaction solution was stirred by a magnetic stirring bar at room temperature for 24 h. After polymerization, the colorless oil was washed with brine 3 times to remove TBD, dried over MgSO_4 , and concentrated by a rotary evaporator. This reaction yielded a colorless oil, i.e., polycaprolactone oligomer, which was then dried at 60 °C under vacuum for 12 h, yielding 46.58 g.



Scheme 1. The synthesis of PCLA.

The obtained polycaprolactone oligomer was reacted with 14.12 g of acryloyl chloride (156 mmol) in 80 mL tetrahydrofuran at 0 °C in an ice bath, using 15.78 g of triethylamine (156 mmol) as the acid scavenger. The slightly yellowish mixture was then stirred at room temperature for another 20 h. After removing the precipitation of triethylamine hydrochloride, the oil was concentrated using a rotary evaporator. The obtained crude product was then dissolved in 300 mL dichloromethane, washed 3 times, and dried over anhydrous MgSO_4 . A slightly yellowish oil was obtained after removing the solvent and dried under vacuum at 30 °C for 24 h, yielding 49.80 g.

2.3. Fabrication of GE Membrane

The comb-like PCL-based GE was prepared via facile in situ radical polymerization inside an argon-filled glove box (H_2O , $\text{O}_2 < 1$ ppm). A mixture composed of 2 g of PCLA,

8 g of LE, and 0.02 g of AIBN was prepared and stirred for 10 min at room temperature in the glove box. The weight fraction of the polymer in the GE was tuned by varying the PCLA/LE ratios. The colorless, clear solution was then poured into a level Teflon Petri dish with a piece of cellulose nonwoven membrane inside. The Teflon Petri dish was sealed to prevent the evaporation of LE while curing at an elevated temperature. A solid, colorless membrane was obtained after curing at 80 °C inside the glove box for 6 h. The GE-based solid-state batteries were all prepared by injecting the PCLA/LE mixture into the cell, sealing the cell case, and curing at 80 °C for 6 h.

2.4. Characterization

The chemical composition of the PCLA was thoroughly studied by proton nuclear magnetic resonance spectroscopy (¹H NMR, Bruker Ascend TM 400 MHz) with CDCl₃ as the solvent and the tetramethylsilane (TMS) as the internal standard. Fourier transform infrared spectroscopy (FTIR) measurement of the PCLA was performed before and after curing on a Nicolet™ iS50 FTIR spectrometer in the wavenumber range of 4000 to 600 cm⁻¹. Microscale observation of the GE film and the lithium electrode surface was conducted using a TESCAN MIRA3 field emission scanning electron microscope.

The electrochemical properties of the GE were all characterized on a Solartron 1260 multichannel potentiostat electrochemical workstation. Electrochemical impedance spectroscopy (EIS) with an AC amplitude of 10 mV was applied to measure the ionic conductivities of the GEs with various LE concentrations in the frequency range of 10⁶ to 10⁻² Hz. In this case, symmetrical SS//SS structured cells with GE sandwiched between stainless-steel sheets (SS) were assembled. The ionic conductivity (σ, S cm⁻¹) was evaluated using Equation (1):

$$\sigma = \frac{L}{R_b A} \quad (1)$$

where L is the thickness of the GE (in cm), R_b is the impedance of the GE (in Ω), and A is the overlapping area of the GE and SS (in cm²).

The oxidation stability of the GE was evaluated using linear sweep voltammograms at 25 °C between 0 V and 7 V vs. Li/Li⁺ at a scanning rate of 1.0 mV s⁻¹. In this case, a stainless-steel sheet was employed as the working electrode, while a metallic lithium sheet was used as the counter and reference electrode.

To measure the lithium-ion transference number (t_{Li}^+) of the GE, a Li/GE/Li symmetrical cell was assembled, and the impedance was tested before and after polarization at room temperature. The t_{Li}^+ value was calculated using Equation (2):

$$t_{Li}^+ = \frac{I_{ss}(\Delta V - I_0 R_0)}{I_0(\Delta V - I_{ss} R_{ss})} \quad (2)$$

where I_0 and I_{ss} denote the initial and stable currents, respectively, and R_0 and R_{ss} denote the interfacial impedance between the GE and the metallic lithium electrodes prior to and following polarization, respectively. The applied DC polarization voltage was 10 mV (ΔV).

The lithium dendrite prohibition property of the GE was evaluated via a galvanostatic cycling study on symmetrical cells of Li/GE/Li on a Shenzhen Neware battery testing system (charged/discharged both for 1 h at 0.1 mA cm⁻²).

The long-term cycling and rate performances of the batteries were tested using a Shenzhen Neware battery testing system. The C-rate was determined according to 1C = 170 mAh g⁻¹, and the applied voltage range was between 2.8 and 3.8 V. A commercial high-loading LiFePO₄ (LFP) cathode was used in our work, with an loading area of ~15 mg cm⁻². All the rate and cycling performance tests were conducted by assembling the LFP/GE/Li structured CR-2032 coin cells.

3. Results and Discussion

3.1. Chemical Characterization

The synthesis of the PCLA precursor was carried out by preparing the PCL oligomer by cationic ring-opening chemistry of ϵ -caprolactone using a strong base, followed by modification of the hydroxy end groups with acryloyl chloride towards PCLA. PCLA was synthesized according to a previously described procedure, as shown in Scheme 1 [14]. The received PCLA precursor was confirmed by an ^1H NMR study, and the proton assignments are depicted in Figure 1.

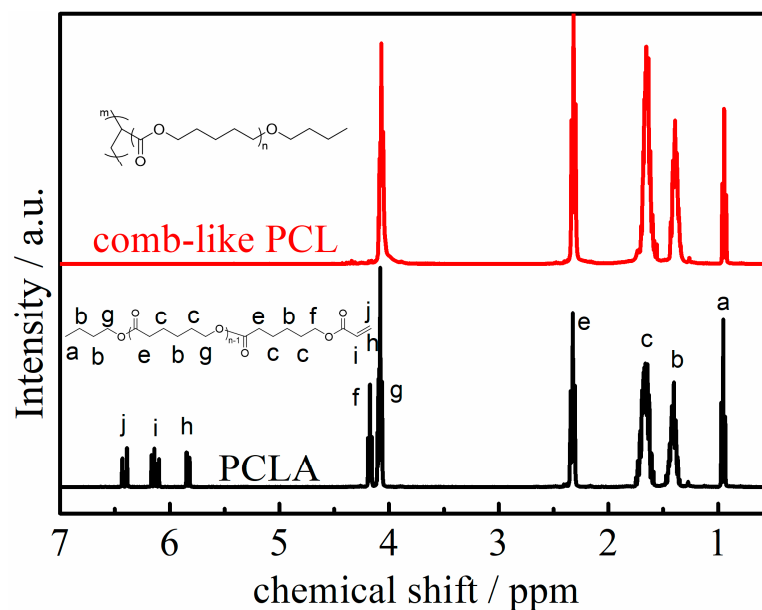


Figure 1. The ^1H NMR results of the PCLA precursor and comb-like PCL in CDCl_3 .

As shown in Figure 1, the proton signals of a (chemical shift, $\delta = \sim 0.95$ ppm), b ($\delta = \sim 1.4$ ppm), and g ($\delta = \sim 4.1$ ppm) are attributed to the 1-butyl end groups from the 1-butanol initiator. The proton signals of c ($\delta = \sim 1.7$ ppm), e ($\delta = \sim 2.3$ ppm), and g ($\delta = \sim 4.1$ ppm) are assigned to $-\text{CH}_2-$, $-\text{CO}-\text{CH}_2-$, and $-\text{CH}_2-\text{O}-$ on the PCLA backbone, respectively. The proton signal of f ($\delta = \sim 4.2$ ppm) is due to the $-\text{CH}_2-\text{O}-$ in the acrylate end functionalities. The proton signals at 5.8 ppm (h), 6.1 ppm (i), and 6.4 ppm (j) are all assigned to the double bonds of the acrylate functionalities. The proton signal assignments confirm the successful synthesis of acrylate-terminated PCLA precursors. According to integration of the peak area of the end groups and the backbone characteristic signals, the average molecular weight (M_n) of the PCLA precursor is $\sim 650 \text{ g}\cdot\text{mol}^{-1}$, which is very close to the theoretical value. The successful preparation of PCLA precursor is also reflected by the FTIR measurements, as shown in Figure 2.

The bands at 1760 cm^{-1} and 1106 cm^{-1} are assigned to the $\text{C}=\text{O}$ stretching vibrations and the $\text{C}-\text{O}$ symmetric stretching vibration, respectively. The characteristic stretching vibration of $\text{C}=\text{C}$ is located at 1638 cm^{-1} , and the deformation vibration of $=\text{C}-\text{H}$ was detected at 1410 and 810 cm^{-1} .

After curing the PCLA and LE mixture into a GE, the chemical structure of the comb-like PCL was confirmed by ^1H NMR and FTIR, as shown in Figures 1 and 2, respectively. In the ^1H NMR spectra of comb-like PCL, the proton signals at 5.8 ppm (h), 6.1 ppm (i), and 6.4 ppm (j) assigned to the double bonds of the acrylate functionalities of PCLA all disappear, indicating the full reaction of the double bonds. This was further confirmed by the disappearance of the proton signal of f ($\delta = \sim 4.2$ ppm) due to the $-\text{CH}_2-\text{O}-$ in the end groups. All other proton signals attributed to the backbone of the PCL oligomer were retained. In the FTIR spectrum of comb-like PCL, the characteristic stretching vibration of $\text{C}=\text{C}$ located at 1638 cm^{-1} totally disappeared, confirming the end-group modification

reaction. The FTIR results are in line with the results of the ^1H NMR experiment, both confirming the successful thermally initiated polymerization of PCLA.

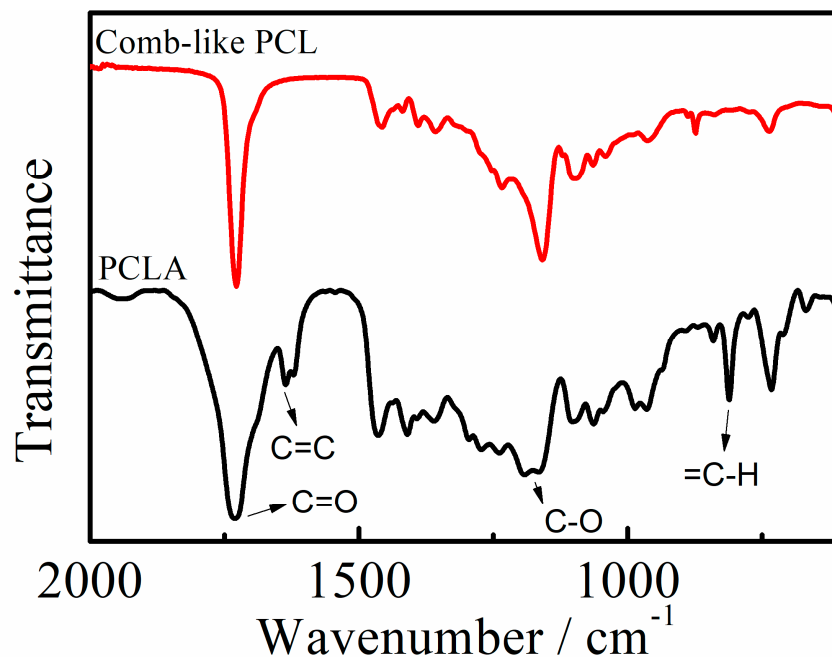


Figure 2. The FTIR results of the PCLA precursor and the comb-like PCL thereof.

3.2. Ionic Conductivity

Sufficient ionic conductivity is the basis for the stable operation of solid-state lithium metal batteries. The ionic conductivity (σ) of the comb-like PCL-based GE as a function of LE contents at 25 °C is depicted in Figure 3.

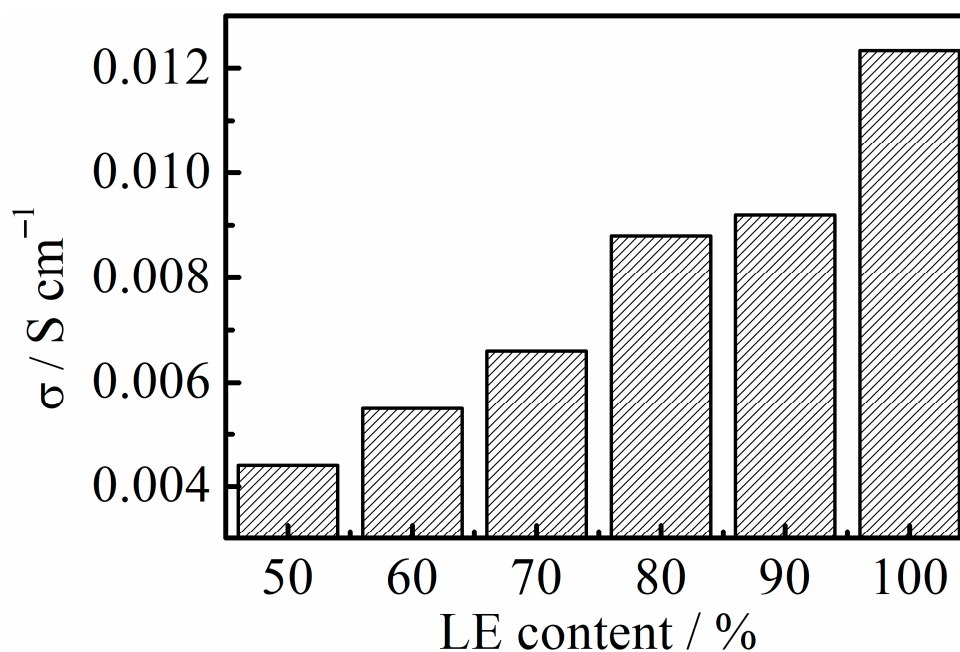


Figure 3. The ionic conductivity of the GE vs. LE contents at 25 °C.

In general, ionic conductivity is enhanced with LE contents, reaching $8.8 \times 10^{-3} \text{ S cm}^{-1}$ at an LE content of 80%. A further increase in the LE proportions does not result in a

significant increase in ionic conductivity. This is clearly due to the fact that the ionic conduction of the LE governs the overall ion transference, even though the comb-like PCL may have some strong interactions with the cations and anions. It should be noted that the ionic conductivity measured in this work was significantly higher than that of other GEs, such as the poly(ether-ester)-based GE reported by Lei et al. [25]. Because the ionic conductivity plateau was first achieved at an LE content of 80%, the GE with an LE content of 80% was chosen for subsequent experiments.

3.3. Morphology of the GE

After the formation of the GE, the facial morphology of the comb-like PCL-based GE membrane with an LE content of 80% was analyzed by scanning electron microscopy (SEM, Figure 4).

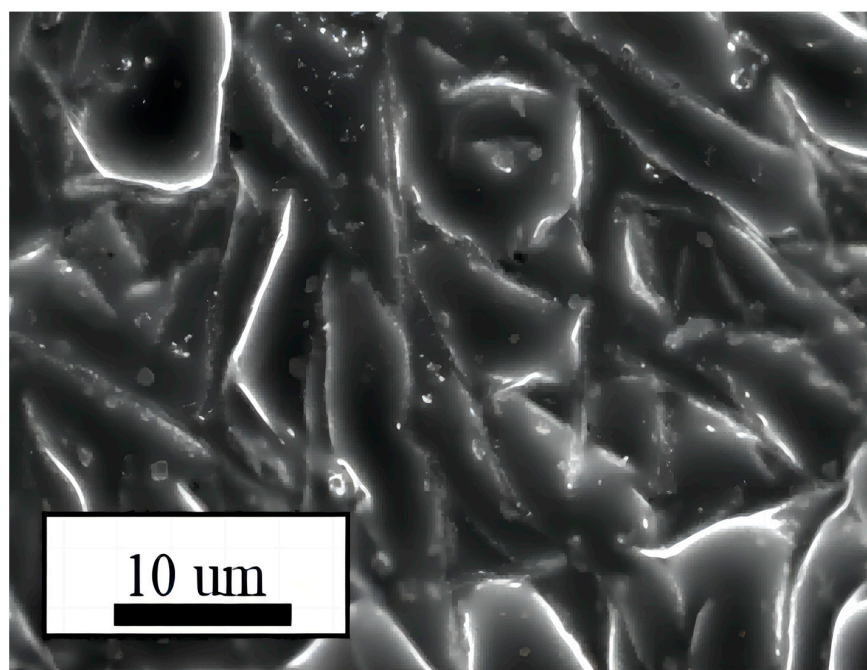


Figure 4. SEM image of the cured comb-like PCL-based GE membrane.

No obvious phase separation was observed, indicating the homogeneous nature of the comb-like PCL-based GE. The SEM image also confirms the complete solvation of LiPF₆ in the GE polymer matrix, with no signs of detectable insoluble lithium salt particles. The comb-like PCL-based GE membrane exhibits no obvious crystalline structure at the microscopic level. The homogeneous nature and high solubility of the lithium salt in the GE highly facilitates the fast transition of lithium ions.

3.4. Electrochemical Stability of the GE

The lithium-ion transference number (t_{Li^+}) of a GE is an essential basis for the battery cycling performance. An ideally high lithium-ion transference number would be close to unity, as it plays an important role in preventing the Li⁺ concentration gradients during battery operation. These Li⁺ concentration gradients are thought to be the cause of various battery defects, including uncontrollable lithium dendrites and charging rate restrictions [26]. In our work, the methodology developed by Evans and Vicent was employed to measure the lithium-ion transference number [27]. The EIS and polarization test results of GE-based Li//Li symmetrical cells are depicted in Figure 5.

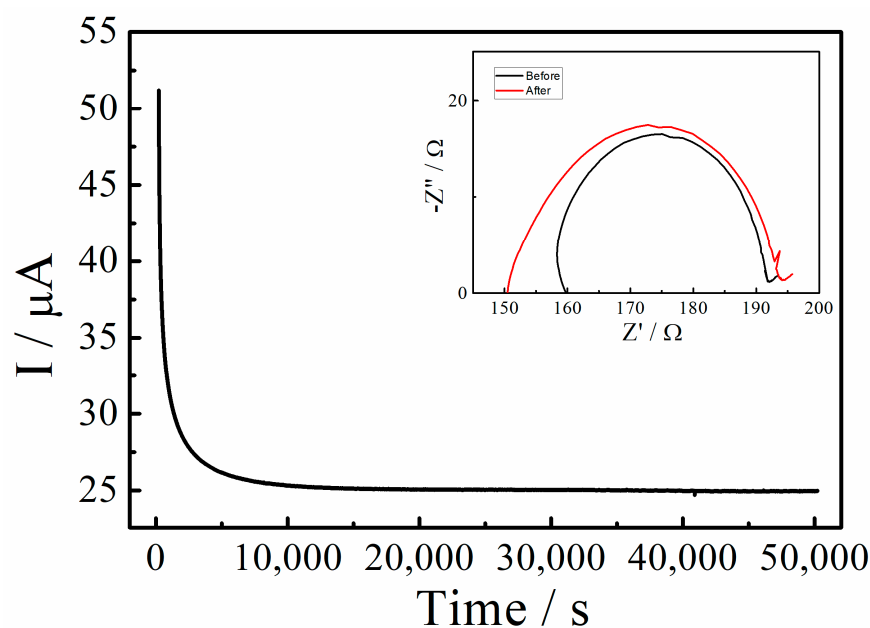


Figure 5. Chronoamperometry of the Li/GE/Li symmetrical cell at 25 °C. The inset shows the AC impedance spectra before and after polarization.

Calculation according to Equation (2) shows that the t_{Li^+} value of the comb-like PCL-based GE is as high as 0.45. In sharp contrast, the t_{Li^+} value of the LE was measured to be only 0.2, which is significantly lower than that of the GE. This is most likely due to the fact that the promotion effect of the polymer matrix on Li^+ ion conduction. In addition, the t_{Li^+} of the GE is also much higher than that of classical polyethylene oxide-based solid-state polymer electrolytes (<0.2) [28,29]. Given that the carbonyl groups in the polymer matrix interact with the Li^+ ions less strongly than polyethylene oxide, the comb-like PCL matrix enables Li^+ transport via a different mechanism [9].

Figure 6 depicts the electrochemical stability results of the comb-like GE as evaluated by linear sweep voltammetry. The in situ polymerized comb-like PCL-based GE exhibits no oxidative decomposition before 5 V in its LSV curve. In sharp contrast, the electrochemical stability of the LE is marginally compromised before 4.6 V. The significant difference in the electrochemical stability of the LE and GE is believed to be derived from the enhancing effect of the polymer matrix. The comb-like polycaprolactone has a polyester skeleton, which has a low HOMO level, thereby enabling a GE with an obviously higher electrochemical stability window. The widely utilized lithium iron phosphate-based cathode ($LiFePO_4$, LFP) has a low electrochemical stability window requirement (working voltage of 3.5 V vs. Li/Li^+) that can be satisfied by the current comb-like PCL-based GE [30].

3.5. Interfacial Stability against Lithium Metal Electrode

The operation performance of solid-state lithium metal batteries is greatly influenced by the interfacial stability between Li and electrolytes [31]. Chronopotentiometry results obtained in the Li plating/stripping test are shown in Figure 7, with a current density of 0.1 mA cm^{-2} and a whole plating/stripping cycle period of 2 h at room temperature. A negative voltage on this curve represents the Li^+ plating, whereas a positive voltage represents the Li^+ stripping. The symmetrical cell using the comb-like PCL-based GE cycles continuously and stably for more than 250 h without experiencing any noticeable negative effects or short circuits. The outstanding performance is most likely due to the excellent adhesive qualities of the in situ polymerized comb-like PCL-based GE, which improved the interfacial contact between the metallic lithium electrodes and the electrolyte membranes [32–34]. In addition, the GE exhibits high t_{Li^+} , which decreases the concentration gradients and polarization [16]. Consequently, lithium dendrite is prohibited. In sharp contrast, the Li//Li symmetrical cells in PEO-based solid-state polymer electrolyte

systems [30] suffer from subpar cycling performances, leading to rapid failure. The in situ polymerized comb-like PCL-based GE investigated in this work significantly improves the interfacial stability of the Li electrode with electrolytes.

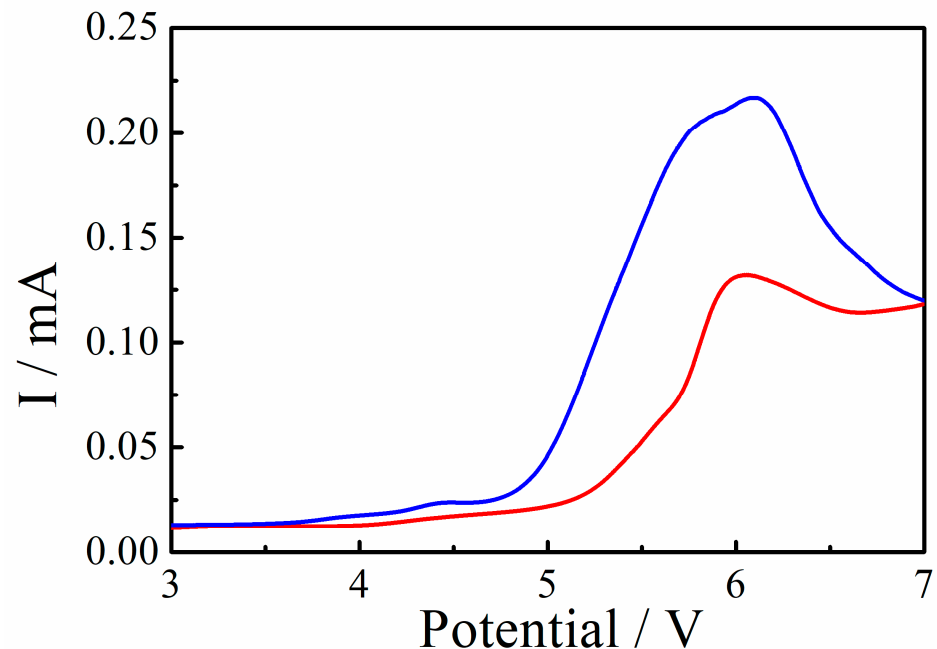


Figure 6. The linear voltammetry curves of the comb-like PCL-based GE (red) and traditional LE (blue) at 25 °C.

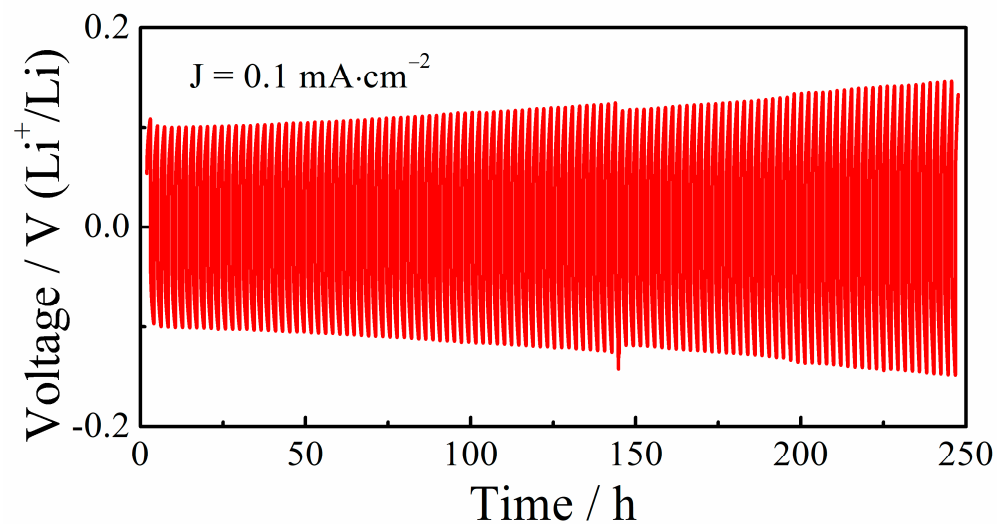


Figure 7. Chronopotentiometry results obtained in the Li plating/stripping test (0.1 mA cm^{-2} , 0.1 mAh cm^{-2}).

3.6. Cell Performance

The rate capacity and cycling performances of the solid-state lithium metal batteries based on the comb-like PCL-based GE were evaluated by assembling LFP/GE/Li cells. To achieve perfect interfacial contact between the GE and cathode, a comb-like PCL-based GE film was fabricated by in situ curing in sealed CR-2032 cells under thermal initiation. Adequate interfacial contact between the GE membranes and the cathodic active materials guarantees the full operational potential of solid-state battery systems [35]. In this study, LiFePO_4 was selected as the cathodic active material due to its superior stability in comparison to other alternatives [36].

In general, the transport efficiency of Li^+ by the solid-state electrolyte itself and the interface between the electrolyte and electrodes play a critical role in determining the rate performance of solid-state batteries.

Figures 8 and S1 show the discharge rate capacity of the LFP/GE/Li solid-state lithium metal batteries, which is based on the in situ cured comb-like PCL-based GE at room temperature and within a voltage range of 2.8 to 3.8 V and a C-rate range of 0.1 to 1C. At a C rate of 0.1C, the cell displays a specific capacity of 149 mAh g^{-1} , which is approximately 93% of the theoretical capacity (160 mAh g^{-1}) of LiFePO_4 [37]. When the charge/discharge current increased to 0.2C, 0.5C, and 1C, the cell displayed reversible discharge capacities of 145 mAh g^{-1} , 139 mAh g^{-1} , and 125 mAh g^{-1} , respectively, which are roughly 91%, 87%, and 78% of the theoretical discharge capacity values, respectively. Throughout testing, the solid-state cell exhibited a Coulombic efficiency of approximately 99%. These experimental results are very promising for solid-state batteries, as they demonstrate a capacity near the theoretical limit of LiFePO_4 at high current rates. This is a significant improvement over the performance of PEO-based solid-state electrolytes, suggesting that the current comb-like PCL-based GE exhibits strong ionic conduction and excellent interface characteristics [38,39]. Finally, when the charge/discharge current was reduced from 1C to 0.1C, the discharge-specific capacity returned to 138 mAh g^{-1} , which is $\sim 93\%$ of its original capacity, indicating strong structural and electrochemical stability.

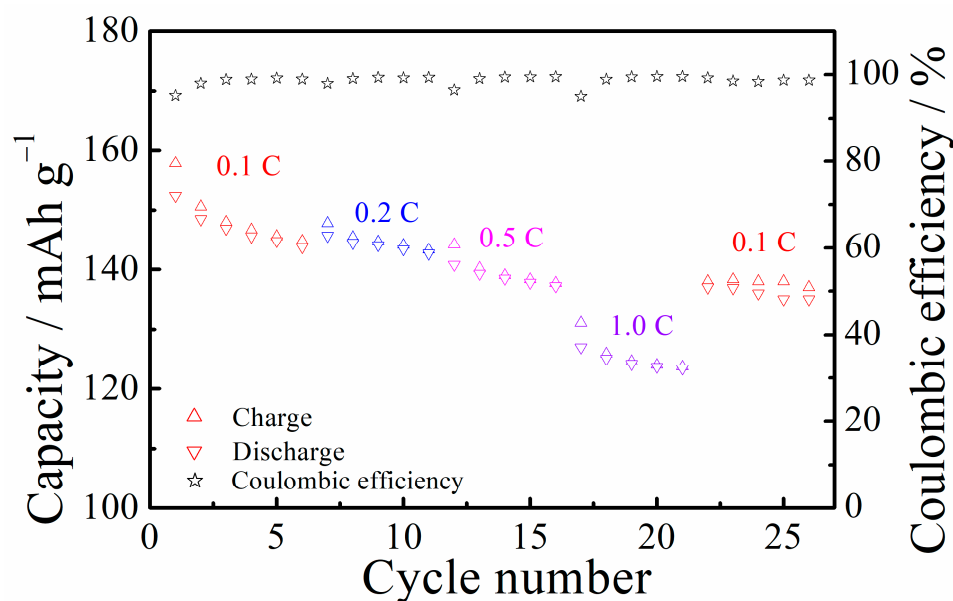


Figure 8. The rate performance of the LFP/GE/Li solid-state battery.

The discharge capacity retention profile of the LFP/GE/Li solid-state lithium metal battery is presented as a function of the cycle number at a C rate of 0.5C in Figures 9 and S2. Basically, the solid-state cell demonstrates remarkable cycling stability at room temperature, with a high initial discharge capacity ($\sim 141 \text{ mAh g}^{-1}$) [40]. After being cycled for 280 cycles, the discharge capacity retention was more than 74% of its initial capacity, with a discharge capacity value of 105 mAh g^{-1} . This excellent performance is attributed to the strong ionic conduction of the GE and effective interfacial contact between the electrodes and the GE generated by the in situ polymerization procedure. Compared with other solid polymer electrolyte-based lithium metal batteries, our GE can be cycled much more stably [34]. However, when the C rate was further increased to 1C, the solid-state battery did not perform very well. This decrease is probably a result of the higher concentration gradient polarization brought about by a high C rate and the limited charge carrier transference kinetics [41].

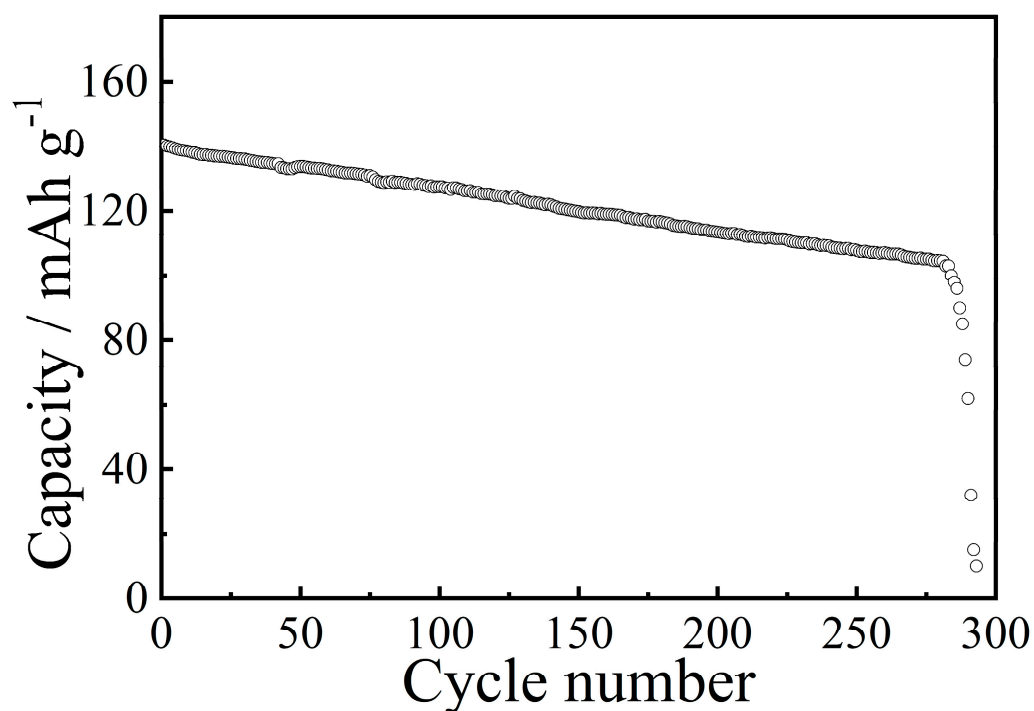


Figure 9. The long-term cycling performance of the GE-based LFP/GE/Li solid-state cell at 0.5C and 25 °C.

4. Conclusions

In conclusion, a new high-performance, comb-like, PCL-based GE was prepared with an acrylate-functionalized PCL precursor and a traditional liquid electrolyte via in situ thermally initiated radical polymerization. The chemical composition and structure of the reactive precursor of the PCLA were confirmed by ^1H NMR and FTIR. SEM observation of the free-standing comb-like PCL-based GE membrane indicated a smooth, homogeneous surface. The GE exhibits a plateau in ionic conductivity ($8.8 \times 10^{-3} \text{ S cm}^{-1}$) with LE content higher than 80%. Compared to the low lithium transference number of ~ 0.2 , the GE shows a high t_{Li^+} of approximately 0.45 due to the improvement effect of the PCL matrix. In addition, the GE displays high electrochemical stability up to 5.0 V vs. Li/Li $^+$. The LiFePO $_4$ /GE/Li cells show extraordinary rate and cycling performance at room temperature, with a superior discharge capacity of 141 mAh g^{-1} and a high capacity retention rate of more than 74% after being cycled for over 280 cycles at a high C rate of 0.5C. The current in situ prepared comb-like PCL-based GE is a promising electrolyte candidate for high-energy, solid-state lithium metal batteries with excellent safety.

Supplementary Materials: The following supporting information can be downloaded at: <https://www.mdpi.com/article/10.3390/ma16052117/s1>.

Author Contributions: Conceptualization, H.W. and Y.F.; methodology, Y.F.; validation, H.W., S.C., and Y.F.; formal analysis, Y.F.; investigation, Y.F.; resources, Y.H.; data curation, Y.F.; writing—original draft preparation, review, and editing, S.W.; visualization, S.W.; supervision, S.W.; project administration, Y.F.; funding acquisition, Y.F. All authors have read and agreed to the published version of the manuscript.

Funding: This research was funded by the Henan Academy of Sciences (No. 220603022).

Data Availability Statement: The data could be provided if it is required by others.

Conflicts of Interest: The authors declare no conflict of interest.

References

1. Goodenough, J.B.; Park, K.-S. The Li-ion rechargeable battery: A perspective. *J. Am. Chem. Soc.* **2013**, *135*, 1167–1176. [[CrossRef](#)] [[PubMed](#)]
2. Xu, W.; Wang, J.; Ding, F.; Chen, X.; Nasybulin, E.; Zhang, Y.; Zhang, J.-G. Lithium metal anodes for rechargeable batteries. *Energy Environ. Sci.* **2014**, *7*, 513–537. [[CrossRef](#)]
3. Eshetu, G.G.; Grugeon, S.; Laruelle, S.; Boyanov, S.; Lecocq, A.; Bertrand, J.-P.; Marlair, G. In-depth safety-focused analysis of solvents used in electrolytes for large scale lithium ion batteries. *Phys. Chem. Chem. Phys.* **2013**, *15*, 9145–9155. [[CrossRef](#)] [[PubMed](#)]
4. Zhou, Q.; Zhang, J.; Cui, G. Rigid–Flexible Coupling Polymer Electrolytes toward High-Energy Lithium Batteries. *Macromol. Mater. Eng.* **2018**, *303*, 1800337. [[CrossRef](#)]
5. Golodnitsky, D.; Strauss, E.; Peled, E.; Greenbaum, S. On order and disorder in polymer electrolytes. *J. Electrochem. Soc.* **2015**, *162*, A2551–A2566. [[CrossRef](#)]
6. Pan, Q.; Smith, D.M.; Qi, H.; Wang, S.; Li, C.Y. Hybrid electrolytes with controlled network structures for lithium metal batteries. *Adv. Mater.* **2015**, *27*, 5995–6001. [[CrossRef](#)]
7. Xu, H.; Zhang, H.; Ma, J.; Xu, G.; Dong, T.; Chen, J.; Cui, G. Overcoming the Challenges of 5 V Spinel LiNi_{0.5}Mn_{1.5}O₄ Cathodes with Solid Polymer Electrolytes. *ACS Energy Lett.* **2019**, *4*, 2871–2886. [[CrossRef](#)]
8. Xue, Z.; He, D.; Xie, X. Poly (ethylene oxide)-based electrolytes for lithium-ion batteries. *J. Mater. Chem. A* **2015**, *3*, 19218–19253. [[CrossRef](#)]
9. Mindemark, J.; Lacey, M.J.; Bowden, T.; Brandell, D. Beyond PEO—Alternative host materials for Li⁺-conducting solid polymer electrolytes. *Prog. Polym. Sci.* **2018**, *81*, 114–143. [[CrossRef](#)]
10. Xu, H.; Xie, J.; Liu, Z.; Wang, J.; Deng, Y. Erratum—Carbonyl-Coordinating Polymers for High-Voltage Solid-State Lithium Batteries: Solid Polymer Electrolytes. *MRS Energy Sustain.* **2020**, *7*, E2. [[CrossRef](#)]
11. Zou, F.; Manthiram, A. A review of the design of advanced binders for high-performance batteries. *Adv. Energy Mater.* **2020**, *10*, 2002508. [[CrossRef](#)]
12. Zhu, Y.; Xiao, S.; Shi, Y.; Yang, Y.; Hou, Y.; Wu, Y. A composite gel polymer electrolyte with high performance based on poly (vinylidene fluoride) and polyborate for lithium ion batteries. *Adv. Energy Mater.* **2014**, *4*, 1300647. [[CrossRef](#)]
13. Luo, W.; Gong, Y.; Zhu, Y.; Li, Y.; Yao, Y.; Zhang, Y.; Fu, K.; Pastel, G.; Lin, C.-F.; Mo, Y.; et al. Reducing interfacial resistance between garnet-structured solid-state electrolyte and Li-metal anode by a germanium layer. *Adv. Mater.* **2017**, *29*, 1606042. [[CrossRef](#)] [[PubMed](#)]
14. Xu, H.; Ye, W.; Wang, Q.; Han, B.; Wang, J.; Wang, C.; Deng, Y. An in situ photopolymerized composite solid electrolyte from halloysite nanotubes and comb-like polycaprolactone for high voltage lithium metal batteries. *J. Mater. Chem. A* **2021**, *9*, 9826–9836. [[CrossRef](#)]
15. Chinnam, P.R.; Zhang, H.; Wunder, S.L. Blends of pegylated polyoctahedralsilsesquioxanes (POSS-PEG) and methyl cellulose as solid polymer electrolytes for lithium batteries. *Electrochim. Acta* **2015**, *170*, 191–201. [[CrossRef](#)]
16. Ye, W.; Zaheer, M.; Li, L.; Wang, J.; Xu, H.; Wang, C.; Deng, Y. Hyperbranched PCL/PS copolymer-based solid polymer electrolytes enable long cycle life of lithium metal batteries. *J. Electrochem. Soc.* **2020**, *167*, 110532. [[CrossRef](#)]
17. Hosseinioun, A.; Paillard, E. In situ crosslinked PMMA gel electrolyte from a low viscosity precursor solution for cost-effective, long lasting and sustainable lithium-ion batteries. *J. Membr. Sci.* **2020**, *594*, 117456. [[CrossRef](#)]
18. Kong, X.; Rudnicki, P.E.; Choudhury, S.; Bao, Z.; Qin, J. Dendrite suppression by a polymer coating: A coarse-grained molecular study. *Adv. Funct. Mater.* **2020**, *30*, 1910138. [[CrossRef](#)]
19. Cheng, X.; Pan, J.; Zhao, Y.; Liao, M.; Peng, H. Gel polymer electrolytes for electrochemical energy storage. *Adv. Energy Mater.* **2018**, *8*, 1702184. [[CrossRef](#)]
20. Wang, S.; Zhou, L.; Tufail, M.K.; Yang, L.; Zhai, P.; Chen, R.; Yang, W. In-Situ synthesized Non-flammable gel polymer electrolyte enable highly safe and Dendrite-Free lithium metal batteries. *Chem. Eng. J.* **2021**, *415*, 128846. [[CrossRef](#)]
21. Park, S.; Jeong, B.; Lim, D.-A.; Lee, C.H.; Ahn, K.H.; Lee, J.H.; Kim, D.-W. Quasi-solid-state electrolyte synthesized using a thiol–ene click chemistry for rechargeable lithium metal batteries with enhanced safety. *ACS Appl. Mater. Interfaces* **2020**, *12*, 19553–19562. [[CrossRef](#)] [[PubMed](#)]
22. Ma, C.; Cui, W.; Liu, X.; Ding, Y.; Wang, Y. In situ preparation of gel polymer electrolyte for lithium batteries: Progress and perspectives. *InfoMat* **2022**, *4*, e12232. [[CrossRef](#)]
23. Wu, S.; Zheng, H.; Tian, R.; Hei, Z.; Liu, H.; Duan, H. In-situ preparation of gel polymer electrolyte with glass fiber membrane for lithium batteries. *J. Power Sources* **2020**, *472*, 228627. [[CrossRef](#)]
24. Niu, C.; Zhang, M.; Chen, G.; Cao, B.; Shi, J.; Du, J.; Chen, Y. An effectively inhibiting lithium dendrite growth in-situ-polymerized gel polymer electrolyte. *Electrochim. Acta* **2018**, *283*, 349–356. [[CrossRef](#)]
25. Chen, Y.; Zhang, Y.; Liang, W.; Xu, H.; Dong, Z.; Xu, J.; Lei, C. In situ-prepared poly (ether-ester)-based gel polymer electrolytes for high-performance lithium metal batteries. *Commun. Chem.* **2022**, *58*, 11961–11964. [[CrossRef](#)]
26. Chazalviel, J.N. Electrochemical aspects of the generation of ramified metallic electrodeposits. *Phys. Rev. A* **1990**, *42*, 7355–7367. [[CrossRef](#)] [[PubMed](#)]
27. Evans, J.; Vincent, C.A.; Bruce, P.G. Electrochemical measurement of transference numbers in polymer electrolytes. *Polymer* **1987**, *28*, 2324–2328. [[CrossRef](#)]

28. Devaux, D.; Bouchet, R.; Glé, D.; Denoyel, R. Mechanism of ion transport in PEO/LiTFSI complexes: Effect of temperature, molecular weight and end groups. *Solid State Ion.* **2012**, *227*, 119–127. [[CrossRef](#)]
29. Devaux, D.; Glé, D.; Phan, T.N.T.; Gignes, D.; Giroud, E.; Deschamps, M.; Denoyel, R.; Bouchet, R. Optimization of block copolymer electrolytes for lithium metal batteries. *Chem. Mater.* **2015**, *27*, 4682–4692. [[CrossRef](#)]
30. Aldalur, I.; Martínez-Ibañez, M.; Piszcz, M.; Rodríguez-Martínez, L.M.; Zhang, H.; Armand, M. Lowering the operational temperature of all-solid-state lithium polymer cell with highly conductive and interfacially robust solid polymer electrolytes. *J. Power Sources* **2018**, *383*, 144–149. [[CrossRef](#)]
31. Cheng, X.-B.; Zhang, R.; Zhao, C.-Z.; Zhang, Q. Toward safe lithium metal anode in rechargeable batteries: A review. *Chem. Rev.* **2017**, *117*, 10403–10473. [[CrossRef](#)]
32. Wei, Z.; Zhang, Z.; Chen, S.; Wang, Z.; Yao, X.; Deng, Y.; Xu, X. UV-cured polymer electrolyte for LiNi_{0.85}Co_{0.05}Al_{0.10}O₂/Li solid state battery working at ambient temperature. *Energy Storage Mater.* **2019**, *22*, 337–345. [[CrossRef](#)]
33. Wei, Z.; Chen, S.; Wang, J.; Wang, Z.; Zhang, Z.; Yao, X.; Deng, Y.; Xu, X. Superior lithium ion conduction of polymer electrolyte with comb-like structure via solvent-free copolymerization for bipolar all-solid-state lithium battery. *Mater. Chem. A* **2018**, *6*, 13438–13447. [[CrossRef](#)]
34. Wang, B.; Lou, H.; Xu, H.; Zhao, J.; Wang, Q.; Shi, Q.; Deng, Y. High voltage, solvent-free solid polymer electrolyte based on a star-comb PDLA-PEG copolymer for lithium ion batteries. *RSC Adv.* **2018**, *8*, 6373–6380. [[CrossRef](#)] [[PubMed](#)]
35. Mindemark, J.; Törmä, E.; Sun, B.; Brandell, D. Copolymers of trimethylene carbonate and ϵ -caprolactone as electrolytes for lithium-ion batteries. *Polymer* **2015**, *63*, 91–98. [[CrossRef](#)]
36. Ellis, B.L.; Lee, K.T.; Nazar, L.F. Positive electrode materials for Li-ion and Li-batteries. *Chem. Mater.* **2010**, *22*, 691–714. [[CrossRef](#)]
37. He, W.; Cui, Z.; Liu, X.; Cui, Y.; Chai, J.; Zhou, X.; Liu, Z.; Cui, G. Carbonate-linked poly(ethylene oxide) polymer electrolytes towards high performance solid state lithium batteries. *Electrochim. Acta* **2017**, *225*, 151–159. [[CrossRef](#)]
38. Appetecchi, G.B.; Hassoun, J.; Scrosati, B.; Croce, F.; Cassel, F.; Salomon, M. Hot-pressed, dry, composite, PEO-based electrolyte membranes: I. Ionic conductivity characterization. *J. Power Sources* **2003**, *124*, 246–253. [[CrossRef](#)]
39. Damen, L.; Hassoun, J.; Mastragostino, M.; Scrosati, B. Solid-state, rechargeable Li/LiFePO₄ polymer battery for electric vehicle application. *J. Power Sources* **2010**, *195*, 6902–6904. [[CrossRef](#)]
40. Eriksson, T.; Gudla, H.; Manabe, Y.; Yoneda, T.; Friesen, D.; Zhang, C.; Inokuma, Y.; Brandell, D.; Mindemark, J. Carbonyl-Containing Solid Polymer Electrolyte Host Materials: Conduction and Coordination in Polyketone, Polyester, and Polycarbonate Systems. *Macromolecules* **2022**, *55*, 10940–10949. [[CrossRef](#)]
41. Wetjen, M.; Navarra, M.A.; Panero, S.; Passerini, S.; Scrosati, B.; Hassoun, J. Composite Poly(ethylene oxide) Electrolytes Plasticized by N-Alkyl-N-butylpyrrolidinium Bis(trifluoromethanesulfonyl)imide for Lithium Batteries. *ChemSusChem* **2013**, *6*, 1037–1043. [[CrossRef](#)] [[PubMed](#)]

Disclaimer/Publisher's Note: The statements, opinions and data contained in all publications are solely those of the individual author(s) and contributor(s) and not of MDPI and/or the editor(s). MDPI and/or the editor(s) disclaim responsibility for any injury to people or property resulting from any ideas, methods, instructions or products referred to in the content.